

EDN: VEETXA

УДК 517.96

Simulation of the Process of Frost Formation on the Surface of the Heat Exchanger Fin

Evgeniy N. Vasil'ev*

Institute of Computational Modelling of SB RAS
Krasnoyarsk, Russian Federation

Received 10.10.2023, received in revised form 28.11.2023, accepted 24.02.2024

Abstract. The paper considers the process of heat and mass transfer during the flow of moist air and formation of frost in the inter-fin space of an air heat exchanger at temperature below 0°C . The mathematical model is based on a system of stationary equations of gas dynamics that describes the flow of moist air in a channel of variable cross section and on a non-stationary system of equations for determining frost deposition on a flat surface. The results of computational modelling of the formation of layer of frost on a surface of a fin with given temperature distribution are presented. It is shown that temperature distribution of the fin surface has a significant influence on frost formation.

Keywords: frost formation, air heat exchanger, heat transfer coefficient, computational modelling.

Citation: E.N. Vasil'ev, Simulation of the Process of Frost Formation on the Surface of the Heat Exchanger Fin, J. Sib. Fed. Univ. Math. Phys., 2024, 17(3), 388–397. EDN: VEETXA.



Introduction

Frost formation is observed on low-temperature surfaces of refrigeration units in contact with moist air. The layer of frost on the working surfaces of air heat exchangers is one of the key factors affecting efficiency of their work. Frost deposition negatively affects the efficiency of refrigeration equipment due to appearance of additional thermal resistance and due to an increase in the hydraulic resistance of the heat exchanger to the air flow when the flow section of the cooled air flow is blocked by frost [1]. Accounting for the processes of frost formation is necessary to choose the design and geometric parameters of finned-plate heat exchangers. Simulation of growth process of the layer of frost allows one to set the optimal operation of the heat exchanger without preventive defrosting.

The design of a thermoelectric cooling unit for ship refrigeration units and results of the study of its characteristics were presented in [2]. The design of an air fin-plate heat exchanger of a thermoelectric cooling unit and results of the study of heat and mass transfer in the exchanger were presented in [3, 4]. Calculation of the temperature field and the heat transfer coefficient of the fin was carried out [3]. It was shown that thermal resistance of the air heat exchanger exerts primary control over cooling capacity and coefficient of performance of the thermoelectric unit. The process of frost formation on the surface of the fins was experimentally studied in [4]. It was established that frost formation has significant effect on heat transfer characteristics. The purpose of this work is to analyse and to model heat and mass transfer processes during formation of frost layer on a flat surface of an air heat exchanger fin.

*ven@icm.krasn.ru <https://orcid.org/0000-0003-0689-2962>
© Siberian Federal University. All rights reserved

1. Computational model of the process of heat and mass transfer in the inter-fin channel

Let us consider the process of heat and mass transfer in the case of a longitudinal flow of moist air around the surface of heat exchanger fins with a temperature below 0°C . The space region is a slit channel with constant cross section, and distance between the fin plates is $2\delta_0$ (Fig. 1). At the initial moment of time the channel is free of frost so the air flows over its entire cross section. When moist air flows on the surface of fins a layer of frost with thickness δ_f is formed. It reduces the height of the passage section of the channel $2\delta = 2\delta_0 - 2\delta_f$. The thickness of the frost layer varies both in time and along the length of the channel. The computational domain is highlighted in the figure by a dashed contour. The computational domain includes zones of the air flow and the frost layer which have movable interface. Let us define systems of equations that describe parameters of the medium in these zones.

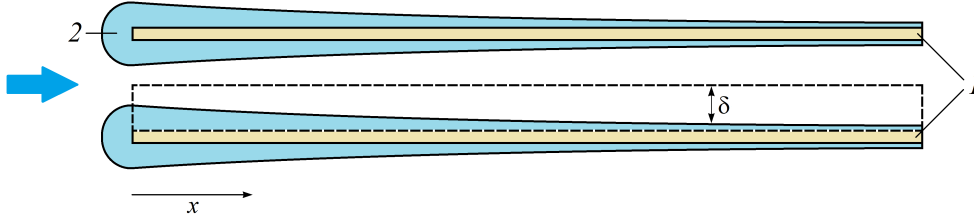


Fig. 1. General view of heat exchanger fins (1) with frost layer (2) and computational domain of the problem (highlighted by a dotted line); the arrow shows the direction of air flow

To describe the flow of moist air consider the system of one-dimensional gas dynamics equations for a channel of variable cross section [5, 6]

$$\frac{\partial(\rho S)}{\partial t} + \frac{\partial(\rho u S)}{\partial x} = 0, \quad (1)$$

$$\frac{\partial(\rho u S)}{\partial t} + \frac{\partial(\rho u^2 S)}{\partial x} + S \frac{\partial p}{\partial x} = 0, \quad (2)$$

$$\frac{\partial(\rho e S)}{\partial t} + \frac{\partial(\rho u e S)}{\partial x} + S \frac{\partial(p u S)}{\partial x} = q_V S, \quad (3)$$

where t – time, ρ , p , e , u – density, pressure, internal energy and air velocity, S – cross-sectional area of the channel. The volumetric capacity of the heat sink q_V is determined by the heat exchange of the air flow with the surface of the frost layer. Equations (1)–(3) are used for gas flows in flat or axisymmetric channels with a slightly changing profile.

Equations (1)–(3) are supplemented with the water vapour mass conservation equation

$$\frac{\partial(\rho_v S)}{\partial t} + \frac{\partial(\rho_v u S)}{\partial x} = -j S, \quad (4)$$

where ρ_v is the vapour density, j is the mass of vapour condensed for 1 s on the surface and recalculated per unit volume of air flow. The effect of vapour in momentum and energy conservation equations is not taken into account because of its negligible contribution ($\rho_v \ll \rho$).

The speed of sound c for the temperature conditions of the refrigerating chamber exceeds 300 m/s and the air flow velocity in the channel $u \leq 3$ m/s. Therefore, the air is considered in

this problem as incompressible medium ($u \ll c$) [7]. In addition, the change in the thickness of the frost layer is the slowest process in the channel. Therefore, the gas-dynamic flow at each moment of time is steady (quasi-stationary) since it quickly adapts to the current profile of the frost layer. Thus, system of equations (1)–(4) is rewritten in the form of a system of ordinary differential equations

$$\frac{d(uS)}{dx} = 0, \quad (5)$$

$$\frac{d(\rho u^2/2 + p)}{dx} = 0, \quad (6)$$

$$\frac{d(c_p T + u^2/2)}{dx} = \frac{q_V}{\rho u}, \quad (7)$$

$$\frac{d\rho_v}{dx} = -\frac{j}{u}, \quad (8)$$

where c_p , T are isobaric heat capacity and air temperature. The boundary conditions for equations (5)–(8) are values of air velocity, pressure and temperature as well as the vapour density in the inlet section of the channel.

The simulation of frost deposition on a flat surface was carried out using a frost growth model based on analytical and empirical relationships [8, 9, 10]

$$\dot{m}_f = \frac{dm_f}{dt} = -\frac{\alpha(\omega - \omega_{fs})}{c_p}, \quad (9)$$

$$\delta_f = \sqrt[3]{\frac{6.34 \cdot 10^{-6} \alpha (\omega - \omega_{fs}) t^2 (T_{fs} - T_p)}{c_p [\alpha (\omega - \omega_{fs}) + 2c_p (T - T_{fs})]}}, \quad (10)$$

$$T_{fs} = T_p + A\beta \left[1 + 0.5\beta \left(0.0196A + \frac{\beta c_f \rho_f}{2c_p \lambda} \right) \right], \quad (11)$$

$$A = \frac{\alpha (T - T_{fs}) \sqrt{t}}{\lambda} \left(1 + \frac{L(\omega - \omega_{fs})}{c_p (T - T_{fs})} \right), \quad (12)$$

$$\rho_f = \frac{m_f}{\delta_f}, \quad (13)$$

$$\lambda = \frac{0.0131 [\exp(0.0196T_{fs} + 273) - \exp(0.0196T_p + 273)] (1 + 0.0134\rho_f)}{T_{fs} - T_p}, \quad (14)$$

where m_f is the specific mass of frost per unit surface of the fin (kg/m^2), α is the heat transfer coefficient of the frost surface ($\text{W}/(\text{m}^2\text{K})$), ω , ω_{fs} – moisture content of air and saturated air at the surface temperature of the frost layer (kg/kg), T_p , T_{fs} – temperature of the fin plate and the surface of the frost layer ($^\circ\text{C}$), ρ_f – frost density (kg/m^3), $\beta = \delta_f/\sqrt{t}$ – frost layer growth factor ($\text{m}/\text{s}^{0.5}$), L – latent heat of sublimation (J/kg). Equations (9)–(14) allow one to calculate the values of m_f , δ_f , T_{fs} for a certain point in time and the current coordinate x for given parameters α , ω , ω_{fs} , T_p and T . The values $\omega = \rho_v/\rho$ and T are calculated from the solution of equations (5)–(8). The value $q_V = \alpha(T_{fs} - T)/\delta$ in (7) is recalculated through surface heat exchange with the layer of frost. The value $j = \dot{m}_f/\delta$ in equation (8) is determined similarly. System of equations (1)–(14) is solved numerically, and distributions of gas-dynamic parameters along the channel are calculated for each time step.

2. Discussion of calculation results

The simulation of heat and mass transfer was carried out for a fin plate length of 0.15 m. Temperature, velocity, and air pressure at the inlet are $T_0 = -10^\circ\text{C}$, $u_0 = 3 \text{ m/s}$, $p_0 = 101 \text{ kPa}$. The air humidity at the inlet $\omega_0 = 1.6 \cdot 10^{-3} \text{ kg/kg}$ is corresponded to the moisture content of saturated air at temperature T_0 . Specified values of parameters approximately correspond to the parameters of the experimental study of frost formation [4]. The temperature distribution along the rib (along the x coordinate) can be uniform or have given profile. The temperature distribution over the fin area can be measured or obtained with the use of computational simulation [3, 11].

One of the most important parameters that affects the process of heat and mass transfer is the heat transfer coefficient of the frost surface α . This parameter is directly present in relations (9), (10), (12), and it implicitly affects the value of q_V on the right side of equation (7). Moreover, the intensity of vapour condensation \dot{m}_f is directly proportional to α . In the initial state, the channel has a constant flow area along the length and the distance between fins is $2\delta_0$. With the growth of the layer of frost the flow area decreases non-uniformly along the length of the fin, and velocity distribution also becomes non-uniform. The value of the heat transfer coefficient of the frost surface α depends heavily on $D=2\delta$, flow velocity and thermophysical properties of the air. Calculation of the heat transfer coefficient for smooth fins of plate heat exchanger with similar process parameters was carried out in [3]. Using the same technique, the relationships between heat transfer coefficient of the surface and inter-fin spacing were obtained for various values of the flow velocity. They are shown in Fig. 2., the curves show the speeds in m/s.

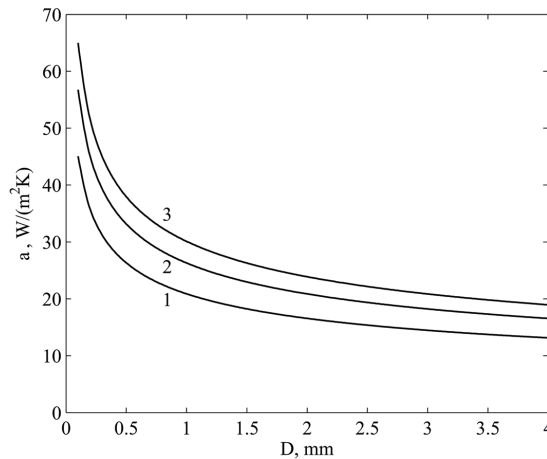


Fig. 2. Relationships between heat transfer coefficient of the surface and inter-fin distance for various values of the flow velocity (values are shown in the graph in m/s)

Function $\alpha(D, u)$ is approximated using interpolation polynomials for use in the computational model. In addition, it is known that heat transfer coefficient of the frost surface differs significantly from the value that corresponds to the smooth surface of the fin. During the formation of frost, the value of heat transfer coefficient α of the surface is affected by the roughness of the frost layer. It was found that in the first hours of frost formation the heat transfer coefficient increases by 1.6–1.8 times in comparison with its value for a smooth metal plate due to surface roughness, and it is 20–25% over its value for a surface without frost in the steady state [12]. To

take this into account in modelling, the value of the heat transfer coefficient of the frost surface was increased by a factor of 1.5 with respect to $\alpha(D, u)$.

The frost formation rate is characterized by the layer thickness $\delta_f(x)$ on the fin surface at different moments of times. The layer thickness as a function of x is shown in Fig. 3 for $\delta_0=1.5$ mm and uniform temperature distribution along the fin $T_p(x) = -20^\circ\text{C}$. Curves correspond to the following moments of time: 1 – 30 min, 2 – 60 min, 3 – 90 min, 4 – 120 min, 5 – 150 min. The most rapid growth of the frost layer occurs near the inlet section where the air flow has a maximum moisture content. As the distance from the inlet section increases the thickness of the frost layer decreases monotonically because vapour content in the flow decreases due to its continuous condensation. Over time, the growth of the frost layer in the downstream part of the channel slows down significantly. This is primarily due to two factors. First, a decrease in the inlet gap $2\delta = 2\delta_0 - 2\delta_f$ due to an increase in the thickness of the frost layer δ_f leads to a proportional decrease in the total mass of steam entering the inter-fin channel. Secondly, faster growth of the frost layer at the inlet leads to a decrease in the downstream flow velocity according to (5) and a corresponding decrease in the heat transfer coefficient which also leads to slowdown in steam condensation. In the inlet part of the channel the heat transfer coefficient increases with an increase in δ_f . This contributes to intense steam condensation. As a result of the combined action of these factors the inhomogeneity of the thickness of the frost layer on the fin increases with time. At time $t = 150$ min, 93% of the cross-section of the channel at the entrance is already blocked by the layer of frost, and only 20% of the output section is blocked. In this inter-fin space an expanding channel is formed in which the air flow velocity decreases from the initial 3 m/s to 0.26 m/s at the outlet.

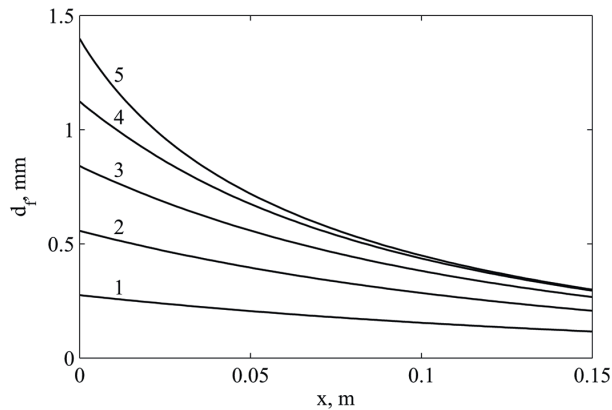


Fig. 3. Frost layer thickness versus x -coordinate at different moments of time: 1 – 30 min, 2 – 60 min, 3 – 90 min, 4 – 120 min, 5 – 150 min

Frost layer thickness δ_f monotonically decreases with x as shown in Fig. 3. This is due to the condensation of steam which leads to steady drop in the moisture content of the air as it moves along the fin. Air humidity $\omega(x)$ as a function of x is shown in Fig. 4 at different moments of time: 1 – 30 min, 2 – 60 min, 3 – 90 min, 4 – 120 min, 5 – 150 min. A decrease in the value of ω leads to a corresponding decrease in the value of the difference $\omega - \omega_{fs}$ which, according to relations (9) and (10), determines the intensity of steam condensation and the thickness of the frost layer. The moisture content of saturated air ω_{fs} depends on the surface temperature of the frost. It is equal to $6.3 \cdot 10^{-4}$ kg/kg at $T = -20^\circ\text{C}$. Curve 5 asymptotically approaches this

value on the chart. Such a sharp decrease in humidity as the inlet section of the inter-fin space is closed is caused by a corresponding decrease in the air flow rate and the mass of steam entering the channel. This small mass of steam is intensively condensed already at the initial section of the fin. Therefore, the air humidity drops significantly over time when approaching the outlet section, and increase in the thickness of the frost layer is insignificant.

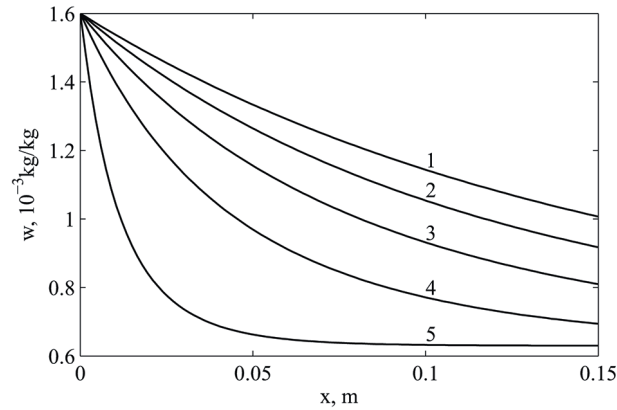


Fig. 4. Air humidity versus x -coordinate at different moments of time: 1 – 30 min, 2 – 60 min, 3 – 90 min, 4 – 120 min, 5 – 150 min

The rate of air cooling in the inter-fin channel of the heat exchanger depends on the difference $T(x) - T_{fs}(x)$. Air temperature as a function of x is shown in Fig. 5. The pattern of $T(x)$ is similar to $\omega(x)$ graphs shown in Fig. 4. This similarity is due to the similar form of relation (9) which describes the process of steam condensation, and the expression for the value of the heat flux coming from the air flow to the frost surface $q = \alpha(T_{fs} - T)$ which determines the value of the air temperature T . As the inlet section of the channel is blocked the outlet temperature approaches the value of the fin temperature.

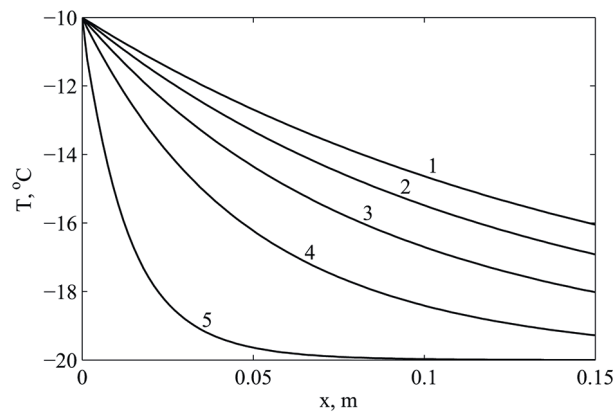


Fig. 5. Air temperature versus x -coordinate at different moments of time: 1 – 30 min, 2 – 60 min, 3 – 90 min, 4 – 120 min, 5 – 150 min

Temperature $T_{fs}(x)$ is determined by the balance of convective heat exchange between the frost surface and the air flow and thermal interaction with the fin surface through the frost layer.

The frost surface temperature as a function of x is shown in Fig. 6 at different moments of time: 1 – 30 min, 2 – 60 min, 3 – 90 min, 4 – 120 min, 5 – 150 min. At the beginning of the process when the thickness of the frost layer is small, the frost surface temperature varies slowly with x , and the value of T_{fs} is close to the temperature of the fin surface. Then, the increase of T_{fs} primarily occurs at the inlet section of the channel due to improved heat exchange with the air flow and decrease in heat flow through the rapidly growing frost layer. Downstream, on the contrary, temperature T_{fs} decreases over time to values close to the temperature of the fin $T_p = -20^\circ\text{C}$ since the air temperature here also has minimum values.

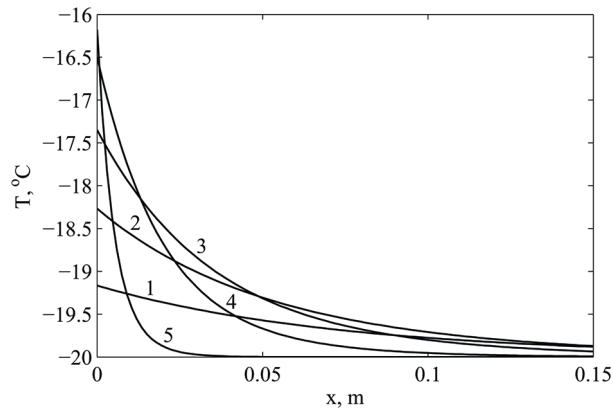


Fig. 6. Frost surface temperature versus x -coordinate at different moments of time: 1 – 30 min, 2 – 60 min, 3 – 90 min, 4 – 120 min, 5 – 150 min

The simulation results for a uniform temperature distribution along the fin showed that the overlap time of the inter-fin gap is determined by the rate of frost deposition on the inlet section. Let us consider the possibility of reducing the intensity of frost formation at the inlet section by changing the temperature profile along the fin. Influence of the temperature distribution of the fin surface on the rate of frost formation was established in experimental study [4]. Thus, in experiments with the orientation of the heat exchanger layout which provides increased temperatures at the initial section of the fin the time of overlapping the inter-fin gap with a layer of frost has significantly increased. To determine the influence of the inhomogeneity of the temperature distribution along the length of the fin $T_p(x)$ calculations were carried out with some model temperature profile. At the same time, the temperature profile in the first third of the channel changes linearly from -16°C at the inlet to -20°C at $x = 0.05$ m, and constant value $T_p = -20^\circ\text{C}$ is set for the rest of the fin. The thickness of the frost layer $\delta_f(x)$ is shown in Fig. 7 at moments of time: 1 – 60 min, 2 – 120 min, 3 – 180 min, 4 – 240 min. Comparing Fig. 3 and Fig. 7, one can see significant effect of the temperature profile of the fin on the rate of the frost layer formation. The inlet section with an increased temperature makes it possible to significantly increase uniformity of the frost deposition along the length of the fin and to reduce the intensity of the frost growth at the inlet. With this temperature distribution, the time for which the channel is almost completely blocked increased from 150 min to 240 min. A similar ratio was observed in experiments [4]. The analysis of $\delta_f(x)$ in Fig. 7 shows that there is still a certain reserve for increasing this time by choosing the optimal temperature profile of the fin.

The efficiency of a heat exchanger is characterized by its ability to remove heat from the air stream. The heat power removed from the air per unit fin width for the two profiles of the fin

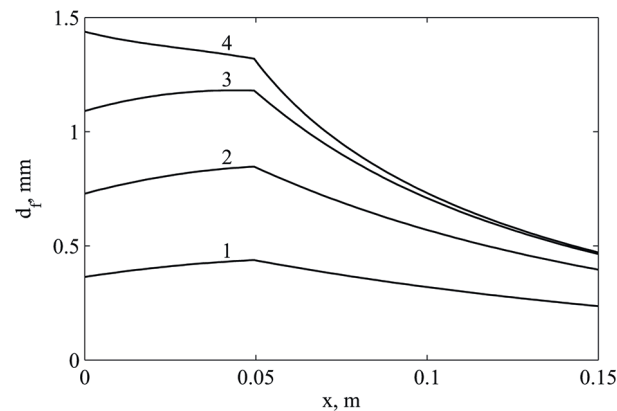


Fig. 7. Frost layer thickness versus x-coordinate at different moments of time with non-uniform temperature distribution: 1 – 60 min, 2 – 120 min, 3 – 180 min, 4 – 240 min

surface temperature considered above is shown in Fig. 8. A fin with a uniform temperature distribution has a slight advantage only for the first 30 minutes then a fin with a non-uniform temperature distribution shows a higher efficiency. It takes 81 minutes to achieve efficiency of at least 70% from the initial heat power for homogeneous profile and 136 minutes for a non-uniform distribution. Thus, setting the temperature distribution of the fin with increased values near the inlet part changes the rate of frost layer formation. It makes deposition of frost more uniform along the length of the fin. As a result, this makes it possible to increase the duration of the effective operation of a heat exchanger and to carry out preventive defrosting procedures less often to remove frost from the surface of fins.

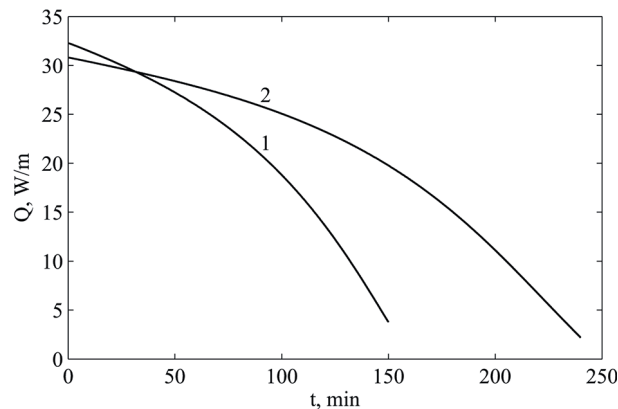


Fig. 8. Thermal power supplied from the air flow to the surface of the frost versus time for uniform (1) and non-uniform (2) temperature distributions along the fin

Conclusion

A computational model is presented to describe the process of frost formation on the surface of an air heat exchanger fin. Frost layer thickness, air temperature and humidity, frost surface

temperature as functions of distance along the fin are obtained. A significant influence of the temperature profile on the rate of frost layer formation and the efficiency of heat exchange between the air flow and the fin surface was revealed. This generally corresponds to patterns identified in the experimental study of the process. Taking into account technical conditions and given operating mode, the proposed computational model can be used to optimize the design of heat exchangers in refrigeration units.

References

- [1] A.A.Gogolin, G.N.Danilova, V.M.Azarskov, N.M.Mednikova, Intensification of heat transfer in evaporators of refrigeration machines, *Legkaya i pishchevaya promyshlennost'*, Moscow, 1982 (in Russian).
- [2] E.N.Vasil'ev, E.R.Geints, V.A.Derevyanko, E.G.Kokov, S.V.Kukushkin, Thermoelectric cooling block. *J. Sib. Fed. Univ. Eng. technol.*, **12**(2019), no. 2, 146–152 (in Russian). DOI: 10.17516/1999-494X-0123
- [3] E.N.Vasil'ev, Calculation and optimization of heat exchangers for a thermoelectric cooling system. *Thermophysics and Aeromechanics*, **29**(2022), no. 3, 401–410. DOI: 10.1134/S0869864322030088
- [4] E.N.Vasil'ev, D.P.Emel'yanov, D.A.Nesterov, Experimental Study of Frost Formation in a Plate Heat Exchanger. *J. Sib. Fed. Univ. Eng. technol.*, **15**(2022), no. 1, 24–34 (in Russian). DOI: 10.17516/1999-494X-0371
- [5] E.A.Kosolapov, M.D.Solennikov, Quasi one-dimensional approach gas flows calculation in power plant channels. *Proceedings of the R.E. Alekseev Nizhny Novgorod State Techn. Univ.*, (2013), no. 5, 60-67 (in Russian).
- [6] E.N.Vasiliev, V.A.Derevyanko, D.A.Nesterov, Numerical modelling of magnetogasdynamic processes in the pulsed setup duct. *Thermophysics and Aeromechanics*, **13**(2006), no. 3, 369–379.
- [7] L.D.Landau, E.M.Lifshits, Theoretical Physics: Hydrodynamics, Nauka, Moscow, 1986 (in Russian).
- [8] B.T.Marinyuk, I.A.Korolev, Calculation and analysis of dynamics of the frost layer growth on a cooled surface. *Kholodilnaya tekhnika*, (2016), no. 11, 38–43 (in Russian).
- [9] B.T.Marinyuk, I.A.Korolev, Thermal conductivity of frost layer as a factor determining heat transfer in chamber cooling systems, *Kholodilnaya tekhnika*, (2017), no. 7, 37–41 (in Russian).
- [10] B.T.Marinyuk, Calculations of heat transfer in apparatus and systems of low-temperature technology, Mashinostroenie, Moscow, 2015 (in Russian).
- [11] E.N.Vasil'ev, Modeling of heat transfer in the heat supply device of the thermoelectric cooling unit, *J. Sib. Fed. Univ. Eng. technol.*, **16**(2023), no. 1, 82–91 (in Russian). EDN: TVIVNX

- [12] В.К.Жавnel', Investigation of the coefficients of heat and mass transfer of a longitudinally streamlined plate during frost formation, *Kholodilnaya tekhnika*, (1968), no. 12, 13–18 (in Russian).

Моделирование процесса инееобразования на поверхности ребра теплообменника

Евгений Н. Васильев

Институт вычислительного моделирования СО РАН
Красноярск, Российская Федерация

Аннотация. В работе рассмотрен процесс тепломассообмена при течении влажного воздуха и образовании инея в межреберном промежутке воздушного теплообменника, имеющего температуру ниже 0°C . Математическая модель основана на системе стационарных уравнений газодинамики для описания течения влажного воздуха в канале переменного сечения и нестационарной системе уравнений для определения динамики осаждения инея на плоской поверхности. Представлены результаты вычислительного моделирования процесса формирования слоя инея на поверхности ребра, имеющего заданное распределение температуры. Показано существенное влияние температурного распределения поверхности ребра на динамику инееобразования.

Ключевые слова: инееобразование, воздушный теплообменник, коэффициент теплоотдачи, вычислительное моделирование.